

Moderate discrimination of REP-1 between Rab7•GDP and Rab7•GTP arises from a difference of an order of magnitude in dissociation rates

Kirill Alexandrov, Iris Simon¹, Andrei Iakovenko, Birgit Holz, Roger S. Goody, Axel J. Scheidig*

Max-Planck Institute for Molecular Physiology, Department of Physical Biochemistry, Rheinlanddamm 201, 44139 Dortmund, Germany

Received 28 January 1998; revised version received 4 March 1998

Abstract The kinetics of the interaction of Rab7 with REP-1 have been investigated using the fluorescence of GDP and GTP analogs at the active site of Rab7. The results show that REP-1 has higher affinity for the GDP bound form of Rab7 ($K_d = 1$ nM) than for the GTP bound form ($K_d = 20$ nM). Both affinities should still be sufficient for the formation of stable complexes in the cell. The association reaction proceeds in two steps for the GDP bound form. The initial step is fast ($k_{+1} = \text{ca. } 10^7 \text{ M}^{-1} \text{ s}^{-1}$) and concentration dependent while the second represents a slow equilibration ($k_{+2} + k_{-2} = 3.5 \text{ s}^{-1}$) which has little effect on the overall equilibrium. The difference in affinity of the two nucleotide bound forms arises from a difference in dissociation rates (0.012 s^{-1} for Rab7•GDP and 0.2 s^{-1} for Rab7•GTP).

© 1998 Federation of European Biochemical Societies.

Key words: Rab7; REP-1; Fluorescence spectroscopy; Kinetics; Small GTP binding protein; Vesicular transport

1. Introduction

The Rab proteins are members of the Ras superfamily of small GTP binding proteins. Many of them have been shown to be involved in the control of intracellular vesicular traffic [1]. They exert their function by switching between a GTP and a GDP bound form [2,3]. For their function Rab proteins require modification by geranylgeranyl isoprenoids. This allows Rab proteins to reversibly associate with the membrane in a controlled fashion [4–6]. The covalent attachment of geranylgeranyl groups to two C-terminal cysteines is catalyzed by the Rab geranylgeranyl transferase (RabGGTase). In contrast to other known prenyl transferases, RabGGTase can recognize its substrate only if it is complexed to another protein termed Rab escort protein (REP) [7–9]. According to current models, a newly synthesized Rab protein forms a stable complex with REP [10,11]. The resulting complex is recognized by RabGGTase, which covalently attaches a geranylgeranyl moiety to the C-terminal cysteines of Rab proteins [12–14]. Upon prenylation the Rab protein remains bound to REP which accompanies it to the corresponding membrane [15,16]. The Rab protein is inserted into the membrane, presumably

through the interaction with a membrane receptor/REP-displacing factor [15,17,18] which might be shared by REP and GDI. Subsequently, REP is released into the cytosol and can enter a new prenylation cycle.

Although the prenylation reaction has been reconstituted in vitro [8,10], only a limited amount of data is available on the interaction of its components at the molecular level. Studies using either mutants of Rab proteins or proteins loaded with nucleotide analogs suggested that the GDP bound conformation of Rab proteins is preferred by RabGGTase [9,19]. However, other investigators came to contradicting conclusions [20]. Despite a number of related reports, the exact affinities of REP-1 for Rab proteins remain unknown and the kinetic mechanism of this interaction is still unexplored. To address this, we have analyzed the interactions between the GTP and GDP bound forms of Rab7 by REP-1 employing fluorescence spectroscopy methods.

2. Materials and methods

2.1. Proteins

Rab7 was expressed in *E. coli* and purified as described previously [21]. In order to obtain the cDNA coding for REP-1 500 ng of total RNA from rat liver (generous gift of Dr. Andreas Werner, Max-Planck Institute, Dortmund) was reverse transcribed using Reverse Transcription System kit (Promega) according to the instructions of the manufacturer. Two μl of the resulting mixture was used for the first rounds of PCR using specific oligodeoxynucleotides 5'-TTAAT-GAAGAACAGGATCCCTTTT-3' and 5'-TCAAGATGCCGGA-TAATCTCC-3' with Expand Polymerase (Boehringer Mannheim). The denaturing, annealing and extension steps were 95°C for 15 s, 55°C for 30 s and 72°C for 2 min with a 20 s increment. The total number of cycles was set to 30. PCR product was purified using a PCR purification kit (Qiagen). After appropriate dilution, 1 μl of PCR product mixture was used as a template for the second round of amplification with adapter oligodeoxynucleotides containing *Nco*I and *Bam*HI restriction sites. The primer sequences were as follows: 5'-GGACGAATCACCATGGCGGATAATCTCCCTTC-3', and 5'-TTAAGTCTGATGCATATCCGATCCTCAGAAAGGCTCTTG-GGTT-3'. The amplification protocol was as above but the annealing temperature was set to 60°C and the number of cycles to 25. The resulting fragment was digested with *Nco*I and *Bam*HI and ligated into modified pET-27b (Novagen) (Iakovenko and Alexandrov, unpublished results). The resulting plasmid, designated pET27-REP, was sequenced and two base exchanges compared to the original sequence (GeneBank accession number L13722) were found. A substitution of C to A at the position 92 resulted in a change of Gly to Lys, a substitution of G to C at the position 1554 resulted in a substitution of Glu to Ala. In order to address the origin of these mutations we sequenced the cDNA clone of REP-1 obtained from American Type Culture Collection (accession number 63224). Sequencing of the corresponding regions revealed that the above mentioned substitutions were also present in that sequence. An insert containing coding sequence of REP-1 with six histidines on the C-terminus was excised from pET27-REP with *Nco*I and *Bpu*1102I and subcloned into modified pBlueHis2 vector (Invitrogen) (Iakovenko and Alexandrov, un-

*Corresponding author. Fax: +49 (231) 1206-229.
E-mail: scheidig@mpi-dortmund.mpg.de

¹Present address: Department of Biochemistry, Stanford University School of Medicine, Stanford, CA 94305-5307, USA.

Abbreviations: Rab, ras like protein from rat brain; GGTase, geranylgeranyl transferase; REP, rab escort protein; mant, *N*-methylanthraniloyl; FRET, fluorescence resonance energy transfer

This work was supported by the Deutsche Forschungsgemeinschaft.

published results). Recombinant baculoviruses expressing REP-1 were generated according to the instructions of the manufacturer (Invitrogen). Recombinant REP-1 used for the kinetic assays was produced in SF9 cells and purified as described [22].

2.2. Nucleotides and nucleotide exchange

N-methylanthraniloyl derivatives (mant) of GDP and GTP were prepared as described [23]. Mant GDP and mant GTP forms of Rab7 were prepared as described earlier [21].

2.3. Fluorescent measurements

Fluorescence spectra and long time base fluorescence measurements were performed with an Aminco SLM 8100 spectrophotometer (Aminco, Silver Spring, MD, USA). All reactions were followed at 25°C in 25 mM HEPES pH 7.2, 40 mM NaCl, 2 mM MgCl₂ and 2 mM DTE. Fluorescence of mant GDP was excited via FRET at 290 nm and measured at 440 nm. For the measurement of the direct fluorescence signal the mant group was excited at 344 nm and data were collected at 440 nm. Stopped flow experiments using mant GDP and mant GTP to monitor the interactions of REP-1 with Rab7 were performed in a High-Tech Scientific apparatus (Salisbury, England). The mant fluorescence was detected by excitation at 344 nm and detected through a 389 nm cutoff filter. Data collection and primary analysis of rate constants were performed with the package from High-Tech Scientific, while secondary analysis was performed with the programs Graft 3.0 (Erithacus software) and Scientist 2.0 (Micro-Math Scientific Software).

3. Results

The use of fluorescent nucleotide analogs is a well established method for analyzing interactions of GTPases with other proteins (e.g. [24]). We tested whether the fluorescence of mant GDP bound to Rab7 changes upon association with REP-1. When the fluorescence of the mant group was excited directly at 344 nm, there was only a small increase in fluorescence on binding of REP-1 to the Rab7-mant GDP complex. This change was too small to be used for accurate titration data. A much larger signal change was seen on binding of REP-1 when the fluorescence of the mant group was excited indirectly by energy transfer from tryptophan. As shown in Fig. 1, there was an easily measured increase in mant fluorescence at 440 nm on excitation at 290 nm on titration with REP-1. The data could be fitted using a quadratic equation

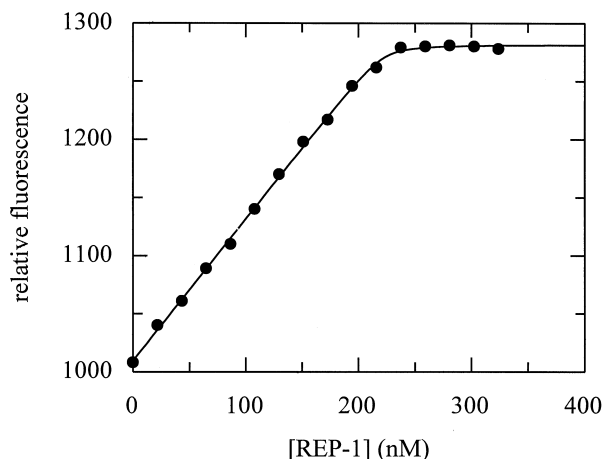


Fig. 1. Titration of REP-1 to a nominal concentration of 250 nM Rab7-mant GDP using fluorescence energy transfer as a signal for binding (excitation wavelength 290 nm, emission 440 nm). The solid line shows the fit to a quadratic equation describing the binding curve and gives a value of 0.44 nM for the K_d and an effective REP-1 concentration of 222 nM.

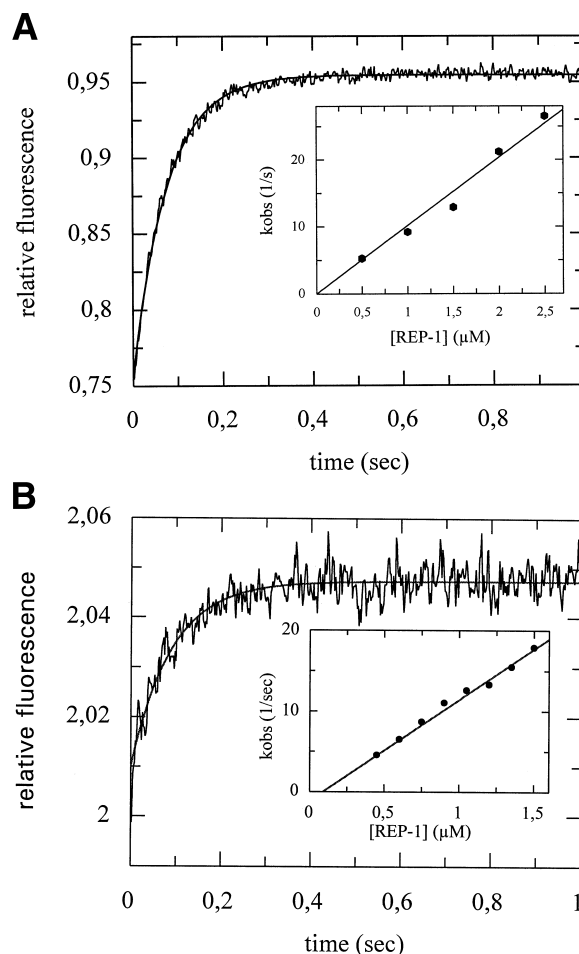


Fig. 2. Time course of the energy transfer signal change seen on mixing (A) Rab7-mant GDP (0.25 μ M) with REP-1 (1.5 μ M) and (B) Rab7-mant GTP (0.15 μ M) with REP-1 (0.9 μ M) in the stopped flow machine. Excitation was at 289 nm, and emission was detected through a 320 nm cutoff filter. The fit shown in A is to a single exponential equation with a rate constant (k_{obs}) of 13.1 s^{-1} . As discussed more extensively later (Fig. 5), there is a slight deviation of the data from the fitted curve, which did not alone, at this point, justify fitting to a more complex model than a single step binding process. The insets show the secondary plot of data from five (A) and eight (B), respectively, experiments of the type shown in the main figure. Since it was not possible to restrict measurements of the binding kinetics to situations which were strictly pseudo-first order (i.e. where REP-1 was in very large excess over Rab7-mant GDP and Rab7-mant GTP, respectively), each transient was analyzed as a second order reaction and the resulting rate constants were used to calculate the theoretical pseudo-first order rate constant at the respective REP-1 concentrations for the case that the concentration of Rab7-mant GDP (or Rab7-mant GTP) was very much smaller. These values of k_{obs} were used for the plot shown in the insets, which gives a value of $1.02 \times 10^7 M^{-1} s^{-1}$ for the association rate constant of Rab7-mant GDP and of $1.25 \times 10^7 M^{-1} s^{-1}$ for the association rate constant of Rab7-mant GTP from the slope of the straight line obtained.

describing the binding curve and were consistent with a 1:1 stoichiometry and a K_d value of 0.44 nM. The K_d value is not very well determined in these experiments, since a concentration of Rab7 had to be used which was considerably higher than the K_d value in order to obtain a stable signal. However, further experiments described below confirm the value obtained.

The change in energy transfer seen on interaction of

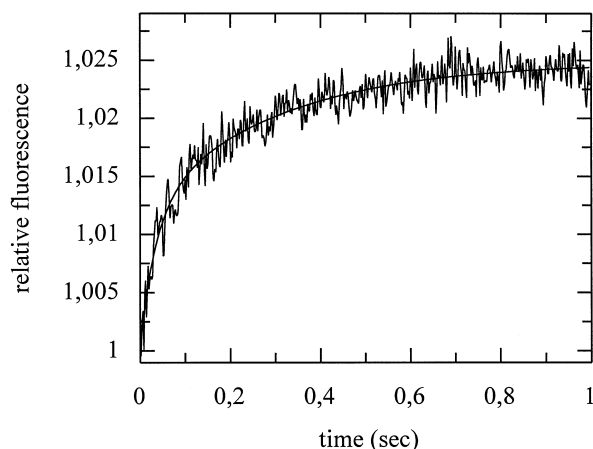


Fig. 3. Time course of the change in fluorescent yield on interaction of Rab7-mant GDP and REP-1 after mixing in the stopped flow machine under the same conditions as in Fig. 2a, except that the mant group fluorescence was excited directly at 365 nm. The solid line shows the result of fitting the constants of the model shown in Eq. 1 using a numerical integration and fitting procedure (Scientist). Rate constant k_{-1} was fixed at the independently measured value of 0.012 s^{-1} , while all other parameters were allowed to vary. The fit obtained was with values of $1.15 \times 10^7 \text{ M}^{-1} \text{ s}^{-1}$ for k_{+1} , 2.5 s^{-1} for k_{+2} and 0.8 s^{-1} for k_{-2} . The amplitude of the fluorescent change for step 1 was 1.1%, for step 2, 1.4%. Similar values were obtained from traces obtained at other concentrations.

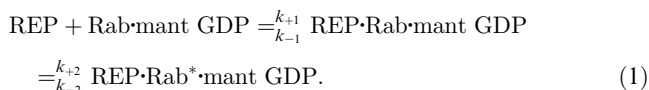
Rab7-mant GDP with REP-1 can also be used to monitor the kinetics of the association reaction. At excess REP-1 concentration, first order conditions were assumed and the transients were evaluated as single exponential curves (Fig. 2). A plot showing the dependence of the pseudo-first order rate constant against the REP-1 concentration is shown in the inset of Fig. 2. The slope of the straight line fitted to the data points defines the second order rate constant, k_{+1} , for association to be $1.02 \times 10^7 \text{ M}^{-1} \text{ s}^{-1}$. The intercept with the y-axis should give the dissociation rate constant, k_{-1} , according to the equation

$$k_{\text{obs}} = k_{+1}[\text{REP} - 1] + k_{-1}.$$

Although it is clear from Fig. 2 (inset) that k_{-1} must be very small, this evaluation does not allow its accurate determination, because of its small magnitude and since the points for low REP-1 concentrations are not very reliable due to the small excess of REP-1.

The value of k_{-1} was determined directly in the following manner. Rab7-mant GDP was mixed with an equimolar amount of REP-1 to a final concentration of $0.25 \mu\text{M}$ and after formation of the ternary complex was mixed with a 10-fold excess of Rab7-GDP. The resulting dissociation of Rab7-mant GDP was monitored using the fluorescence energy transfer signal. The resulting time course could be fitted as a single exponential curve, leading to a value of $0.012 \pm 0.001 \text{ s}^{-1}$ for the dissociation rate of REP-1. Together with the measured association rate, this allowed calculation of the dissociation constant of Rab7-mant GDP-REP-1, which is estimated to be ca. 1 nM based on these results. This agrees quite well with the somewhat uncertain value obtained from the direct titration (Fig. 1).

If the fluorescence of the mant group was excited directly to monitor association kinetics, the signal was much noisier but was clearly not single exponential (Fig. 3). The data could be fitted as the sum of two exponentials in which the first phase was concentration dependent and the second was constant at ca. 3 s^{-1} . A more appropriate method of analysis was to use a numerical integration and fitting procedure using the set of differential equations describing the time dependence of the two-step binding reaction shown in the following scheme:



The data can only be explained if we assume that the value of 0.012 s^{-1} obtained for the rate of dissociation of the Rab7-mant GDP-REP complex corresponds to k_{-1} , and that fluorescence changes occur in both steps of the mechanism. The values obtained from the fitting procedure are given in the legend to Fig. 3, and it can be seen that the value of k_{+1} agrees well with that obtained from the data of Fig. 2. The individual values of k_{+2} and k_{-2} are not well determined,

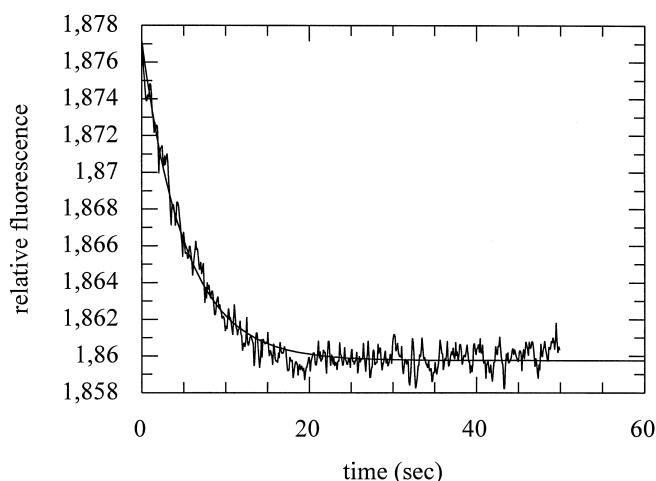


Fig. 4. Time course of the energy transfer signal change seen on mixing Rab7-mant GTP-REP-1 ($0.25 \mu\text{M}$) with Rab7-GDP ($2.5 \mu\text{M}$) in the stopped flow machine. Excitation was at 289 nm, and emission was detected through a 320 nm cutoff filter. The fit shown is to a single exponential equation with a rate constant k_{-1} for the displacement of Rab7-mant GTP with Rab7-GDP of 0.2 s^{-1} .

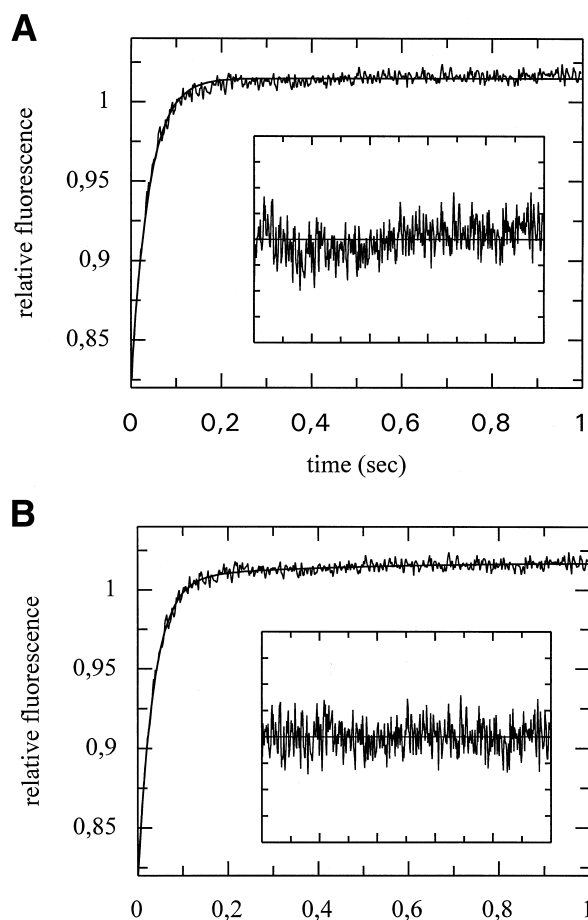


Fig. 5. Comparison of single (A) and double (B) exponential fits to the fluorescence transient obtained on mixing $0.25 \mu\text{M}$ Rab7-mant GDP with $2.5 \mu\text{M}$ REP-1. The insets show the residuals (difference between the experimental and calculated data) as a function of time. It can be seen that the double exponential fit is better than the single exponential fit. Constants obtained were 25 s^{-1} for the single component in A, and 28.2 and 2.7 s^{-1} for the two components in B. The relative amplitude of the second phase was 5.8% of the first phase. The data could also be analyzed as in Fig. 3 using the program Scientist. This led to values of $1.18 \times 10^6 \text{ M}^{-1} \text{ s}^{-1}$ for k_{+1} and 2.15 for k_{+2} .

since the data only contain real information on the sum of the rate constants, which determines the rate of equilibration of the second step. However $k_{+2} + k_{-2}$ is well determined, and was seen to be ca. 3.3 s^{-1} in several experiments at different concentrations of reagents. It is likely that k_{+2} and k_{-2} are of similar magnitude to agree with the fact that the energy transfer signal was essentially single exponential, even at low concentrations of REP-1 and because the agreement between the overall K_d calculated from the kinetic constants and the value and that obtained by direct titration were in agreement.

In the light of these results, the energy transfer data (Fig. 4) were reexamined more carefully, since it seemed unlikely that a change in fluorescence can occur in the second step with no change at all in energy transfer, although this is not completely excluded. It was noted that there is in fact a slight deviation from exponential behavior in all curves obtained, and considerably better fits can be obtained using a double exponential equation. As shown in Fig. 5, at $1.5 \mu\text{M}$, the values for the two phases were 28.2 s^{-1} and 2.7 s^{-1} , which are quite similar to those obtained from the direct fluores-

cence data. However, the amplitude of the second phase is only ca. 6% of the first phase, whereas the two phases are of similar amplitude for direct fluorescence. This is the reason for the greater difficulty of detection of the second phase.

It should be pointed out that, in general, two-step binding mechanisms can also involve a pre-binding equilibration of one of the two components followed by a second order binding step rather than the mechanism shown in Eq. 1, in which the second order association reaction is followed by a first order isomerization reaction. However, in the case reported here, the results obtained exclude the pre-binding equilibration mechanism, since at high concentrations of reagents, a concentration dependent rapid association phase is followed by an essentially concentration independent slow phase. If the slow phase corresponded to equilibration of one of the components, the rapid second phase would not be observed. We can also exclude the possibility that the two phases seen are due to different behavior of the mixture of isomers of mant GTP (2'-O and 3'-O derivatives) used. In this case, two phases which are both concentration dependent would be expected, in contrast to the situation described in which a faster concentration dependent phase is followed by a slower concentration independent phase.

To compare the affinities of the GTP and GDP bound forms of Rab7 for REP-1, we repeated the same set of experiments with the Rab7-mant GTP complex. The increase of the fluorescence signal with energy transfer was about 4% , i.e. much smaller than for Rab7-mant GDP, and there was no detectable change by direct fluorescence. Using the same procedure as for Fig. 2, the association rate constant was estimated to be $1.25 \times 10^7 \text{ M}^{-1} \text{ s}^{-1}$, very similar to that of the GDP bound form of Rab7. However, the dissociation rate constant determined for the Rab7-mant GTP-REP-1 complex by displacement with Rab7-GDP (see Fig. 4) was found to be 0.2 s^{-1} , or more than an order of magnitude greater than for Rab7-mant GDP. The calculated K_d was therefore ca. 20 nM . The difference in the affinities for the GTP and GDP bound conformations is in the range of that obtained earlier for the Rab1-REP-1 interaction where a 10–50-fold difference was observed [10].

4. Discussion

We have investigated the interaction of REP-1 with the GDP or GTP bound forms of Rab7. With Rab7-GDP, the binding reaction appears to proceed in at least two steps. The studies performed revealed a second order process which leads to a complex which is already very stable, followed by a slow step of relatively low equilibrium constant which cannot be analyzed in detail at present. The K_d for the GDP bound form of Rab7 is ca. 1 nM , while that of the GTP form is ca. 20 nM . For the GTP bound form, only one step could be identified in the binding reaction, and the change in fluorescence properties of the labelled nucleotide was considerably smaller than that in the case of GDP, suggesting a structural difference in the two ternary complexes. An intriguing question concerns the affinity of prenylated Rab7 for REP-1. The example of RabGDI suggests that prenylated forms of Rab proteins should interact much more strongly than unprenylated forms with REP-1. This in turn would mean that a putative membrane acceptor must possess an efficient mechanism for dissociating

this complex and transferring the Rab protein onto a membrane. It is also imaginable that upon prenylation a conformational change occurs that weakens the protein:protein interaction and the complex is held together mainly by hydrophobic lipid:protein interactions. Such interactions would be much more sensitive to changes in the hydrophobicity of the environment and could be weakened, for example, by contact with a lipid bilayer.

We have shown that REP-1 has a lower affinity for the GTP bound form of Rab7 than for the GDP bound form. The 20-fold observed affinity difference between these conformations corresponds with and extends earlier data obtained for the Rab1a·REP complex [10]. The ability to discriminate between GDP and GTP bound conformations of Rab proteins is shared between RabGDIs and REPs [25]. It is likely that one of the REP/GDI binding regions is located in the part of the Rab molecule that assumes a different conformation depending on the bound nucleotide. The effector loop is one out of four regions proposed to be involved in Rab·REP-1 interaction [20]. It undergoes conformational changes upon nucleotide exchange and hence seems to be a most likely candidate for this role [26].

It should be noted that the K_d value of 20 nM for the GTP bound conformation should still be sufficient to keep Rab7·GTP and REP-1 in a stable complex. This finding, however, contradicts earlier data that the GTP bound form of Rab1a does not form a stable complex with REP-1 [10]. One possible explanation is that different Rab proteins have different affinities for REP-1. Preliminary data indicated that the Rab1a·GDP·REP-1 complex has a K_d in a range of 200 nM [25]. In this case, a 20-fold affinity difference would result in a K_d of 4 μ M for Rab1a·GTP·REP-1 complex. This affinity could be too low for a complex to be detected in the precipitation assays used by the authors [27]. The difference in absolute affinity might also arise from the influence of the polyhistidine tag used in the case of Rab1a [10]. It is conceivable that addition of the six polar amino acids to the N-terminus perturbs the Rab·REP interactions, since it has been demonstrated that the N-terminus is important for the function of Rab5 protein [28].

If, as in the case of Rab7, the formation of the Rab·REP complex is not critically dependent on the nucleotide bound conformation of the Rab protein, it can be speculated that the difference in the prenylation efficiency is due to different interactions with RabGGTase. The interaction of the Rab·REP complex with RabGGTase remains largely unexplored and hence the possibility remains that the transferase itself distinguishes between the GTP and GDP conformations. Further experiments will be necessary to test this hypothesis.

Acknowledgements: We are grateful to Andrea Beste for synthesis of the nucleotides and technical support. We also thank Angela Wan-

dinger-Ness (Northwestern University, Evanston, IL) for Rab7 expression construct.

References

- [1] Novick, P. and Zerial, M. (1997) *Curr. Opin. Cell Biol.* 9, 496–504.
- [2] Stenmark, H., Parton, R.G., Steele-Mortimer, O., Lutcke, A., Gruenberg, J. and Zerial, M. (1994) *EMBO J.* 13, 1287–1296.
- [3] Rybin, V., Ullrich, O., Rubino, M., Alexandrov, K., Simon, I., Seabra, C.M., Goody, R. and Zerial, M. (1996) *Nature* 383, 266–269.
- [4] Regazzi, R., Kikuchi, A., Takai, Y. and Wollheim, C.B. (1992) *J. Biol. Chem.* 267, 17512–17519.
- [5] Ullrich, O., Stenmark, H., Alexandrov, K., Huber, L.A., Kaibuchi, K., Sasaki, T., Takai, Y. and Zerial, M. (1993) *J. Biol. Chem.* 268, 18143–18150.
- [6] Soldati, T., Riederer, M.A. and Pfeffer, S.R. (1993) *Mol. Biol. Cell* 4, 425–434.
- [7] Shen, F. and Seabra, M.C. (1996) *J. Biol. Chem.* 271, 3692–3698.
- [8] Andres, D.A., Seabra, M.C., Brown, M.S., Armstrong, S.A., Smeland, T.E., Cremers, F.P. and Goldstein, J.L. (1993) *Cell* 73, 1091–1099.
- [9] Seabra, M.C., Brown, M.S., Slaughter, C.A., Südhof, T.C. and Goldstein, J.L. (1992) *Cell* 70, 1049–1057.
- [10] Seabra, M.C. (1996) *J. Biol. Chem.* 271, 14398–14404.
- [11] Casey, P.J. and Seabra, M.C. (1996) *J. Biol. Chem.* 271, 5289–5292.
- [12] Robinson, M.S., Watts, C. and Zerial, M. (1996) *Cell* 84, 13–21.
- [13] Horiuchi, H., Giner, A., Hoflack, B. and Zerial, M. (1995) *J. Biol. Chem.* 270, 11257–11262.
- [14] Lutcke, A., Olkkonen, V.M., Dupree, P., Lutcke, H., Simons, K. and Zerial, M. (1995) *Gene* 155, 257–260.
- [15] Alexandrov, K., Horiuchi, H., Steele-Mortimer, O., Seabra, M.C. and Zerial, M. (1994) *EMBO J.* 13, 5262–5273.
- [16] Wilson, A.L., Erdman, R.A. and Maltese, W.A. (1996) *J. Biol. Chem.* 271, 10932–10940.
- [17] Dirac-Svejstrup, A.B., Soldati, T., Shapiro, A.D. and Pfeffer, S.R. (1994) *J. Biol. Chem.* 269, 15427–15430.
- [18] Soldati, T., Shapiro, A.D. and Pfeffer, S.R. (1995) *Methods Enzymol.* 257, 253–259.
- [19] Sanford, J.C., Pan, Y. and Wessling-Resnick, M. (1995) *Mol. Biol. Cell* 6, 71–85.
- [20] Beranger, F., Cadwallader, K., Porfiri, E., Powers, S., Evans, T., de Gunzburg, J. and Hancock, J.F. (1994) *J. Biol. Chem.* 269, 13637–13643.
- [21] Simon, I., Zerial, M. and Goody, R.S. (1996) *J. Biol. Chem.* 271, 20470–20478.
- [22] Cremers, F.P., Armstrong, S.A., Seabra, M.C., Brown, M.S. and Goldstein, J.L. (1994) *J. Biol. Chem.* 269, 2111–2117.
- [23] John, J., Sohmen, R., Feuerstein, J., Linke, R., Wittinghofer, A. and Goody, R.S. (1990) *Biochemistry* 29, 6058–6065.
- [24] Klebe, C., Prinz, H., Wittinghofer, A. and Goody, R.S. (1995) *Biochemistry* 34, 12543–12552.
- [25] Araki, S., Kikuchi, A., Hata, Y., Isomura, M. and Takai, Y. (1990) *J. Biol. Chem.* 265, 13007–13015.
- [26] Wilson, A.L. and Maltese, W.A. (1993) *J. Biol. Chem.* 268, 14561–14564.
- [27] Newman, C.M. and Magee, A.I. (1993) *Biochim. Biophys. Acta* 1155, 79–96.
- [28] Steele-Mortimer, O., Clague, M.J., Huber, L.A., Chavrier, P., Gruenberg, J. and Gorvel, J.P. (1994) *EMBO J.* 13, 34–41.